CONF-890736--64

3-D Heat Transfer Computer Calculations of the Performance of the IAEA's Air-Bath Calorimeters *

E. Elias and S. Kaizermann
Department of Nuclear Engineering
Technion - Israel Institute of Technology, Haifa 32000, Israel

CONF-890736--64

DE89 016908

R. B. Perry
Argonne National Laboratory
Argonne, Illinois 60439

S. Fiarman
Brookhaven National Laboratory
Upton, New-York 11973

Abstract

A three dimensional (3-D) heat transfer computer code was developed to study and optimize the design parameters and to better understand the performance characteristics of the IAEA's air-bath calorimeters. The computer model accounts for heat conduction and radiation in the complex materials of the calorimeter and for heat convection and radiation at its outer surface. The temperature servo controller is modelled as an integral part of the heat balance equations in the system. The model predictions will be validated against test data using the ANL bulk calorimeter.

1 Introduction

Calorimetry provides an accurate and reliable mean for quantitative non-destructive analysis of heat generating materials. Calorimeters are widely used for measuring the amount of plutonium in small samples and in large containers generating up to 40 Watt of heat [1-5]. They are relatively insensitive to matrix and inhomogeneity effects provided the isotopic composition (or the effective specific power) of the sample is known [6].

Calorimetry has been applied to a wide variety of Pu-bearing solids including metals, alloys, oxides, fluorides, mixed U-Pu oxides and scrap. Accurate measurement of 20 Watt Pu samples to better than 0.2 percent precision are reported [3], using servo-controlled, fixed temperature systems. However, high accuracy measurements are slow as they require the system to stabilize before the sample power is determined. The approach to equilibrium is a function of several processes with different time constants related to the thermal properties of the source, the container, the calorimeter chamber, the insulator etc. A typical time to reach new steady state conditions following the introduction of a heat generating sample is 2-6 hours. Measurement of one or more standards a week as a measurment control further reduces the throughput. Therefore, a fast calorimetry technique was recently proposed [7,8] wherby a well preheated plutonium bearing samples could be measured in about 15 min with a precision of a few percent. An advanced calorimeter system specifically designed for fast calorimetry is being built and this modelling program will be utilized to optimize the design parameters of the system. To test the model's system algorithm, data from an existing 20-Watt and 40-Watt calorimeter will be used [8,9]. During calibration, the larger calorimeter exhibited small heat distribution errors. The test results were found to be sensitive to the location of the sample within the calorimeter chamber. These discrepencies were attributed to small uncontrolled heat losses through the insulation materials. Hence, a three-dimensional computer code was developed to better understand the design and performance of these calorimeters. The model simulates the calorimeter and the preheater geometry and materials as well as the servo-controller loops. In addition, the code was used to simulate a number of design and operational conditions which influence the time constant of the system. Among these are the construction material properties, the preheating duration, the source spatial distribution and the gain coefficients of the power control system.

This paper describes the computer simulation model. bulk calorimeter. The sensitivity of the results to several design parameters and operational conditions are discussed. It should be noted that the simulation code and the physical observation made are not limited to a specific calorimetric system.

*Work supported by the U. S. Department of Energy, Office of Safeguards and Security, under Contract W-31-109-Eng-38.

2 Physical–Mathematical Model and Computational Strategy

The behavior analysis of the system under consideration (calorimeter and preheater) involves the solution of the transient, two–dimensional (at least) general heat transport equation coupled with a closed loop automatic control model. The heat transport equation is given by:

$$\rho c \frac{\partial T}{\partial t} = -\underline{\nabla} \cdot \underline{q} + Q''' \tag{2.1}$$

where T, ρ, c, $\underline{q}$, and Q''' are temperature, density, specific heat,heat flux vector and body heating per unit volume respectiveiy. The heat flux vector may include the effect of all heat transfer mechanisms, i.e., conduction, convection and radiation. The body source term has two components:

$$Q''' = Q'''_e + Q'''_N \tag{2.2}$$

Q'''_e is the electrical source term per unit volume which is constantly updated by the control system simulation and Q'''_N is the heat generation per unit volume due to nuclear radiation.

The electrical power is derived by a proportional–integral–differential (PID) controller defined by the following equation:

$$\frac{1}{Q'''_e}\frac{dQ'''_e}{dt} = k_p \frac{dD}{dt} + \frac{k_i}{t_i} D + k_d t_d \frac{d^2 D}{dt^2} \tag{2.3}$$

where k_p, k_i and k_d are the proportional, integral and differential sensitivity coefficients (in 1/°K) respectively. t_d and t_i are the derivative and integral time respectively. The deviation variable, D, is defined as

$$D = T_r - T \tag{2.4}$$

where T_r is a reference (set-point) temperature.

The physical model equations (2.1 - 2.4) are solved by an integral method–control volume approach [10]. The domain of interest is divided into an arbitrary number of control volumes (CV), each being characterized by its geometrical dimensions, its representative temperature, thermal properties and heat generation rate. The heat transfer equation is first integrated over each CV. Using the divergence theorem, the volume integral of the first term on the right hand side of eq. (2.1) is transformed into a surface integral of heat fluxes over the CV's faces. The heat flux vector, at the faces, is related to the gradient of temperature by the Fourier law, Newton's cooling law, or by the Stefan-Boltzmann law if respectively conduction, convection, or radiation heat transfer mechanicsm occurs at that face [11]. Any combination of heat transfer modes, as may practically exists, can be simulated. Integrating again eq. (2.1) over time from t to $t + \Delta t$ we finally obtain for each control volume, i, the following finite difference equation

$$(\rho c V)_i^n \frac{T_i^{n+1} - T_i^n}{\Delta t} = \sum_j \{(k'A)_{\text{cond}} + (hA)_{\text{conv.}} + \left[\epsilon\sigma(T_{ii} + T_i)(T_{ii}^2 + T_i^2)A\right]_{\text{rad.}}\}_{ij}^n \left(T_{ii}^{n+\ell} - T_i^{n+\ell}\right) + Q_{e,i}^{n+1} + Q_{N,i}^{n+1} \tag{2.5}$$

Here V denotes the volume of the CV, h an average convective heat transfer coefficient, ϵ the product of the emissivity and a form factor, σ the Stefan-Boltzmann constant and k' an equivalent thermal conductivity per unit length at the interface between two control volumes, given by eq. (2.6). The subscript ij denotes the face j between volume i and the adjacent CV ii. k' is calculated as:

$$k'_{ij} = \frac{k_i k_{ii}}{L_{i,j} k_{ii} + L_{ii,j} k_i} \tag{2.6}$$

where $L_{i,j}$ and $L_{ii,j}$ are the distances from the centers of the adjacent volumes i and ii to their common interface ij, respectively.

The superscripts $n+1$ and n denote that the quantity is evaluated at the new time $t + \Delta t$, or the old time, t, respectively. The index ℓ in the superscript $n + \ell$ may be 0 or 1 meaning that an explicit or implicit numerical method can be used for the solution of the heat transport equation. The stability restriction, if the explicit numerical method is used, limits the magnitude of the time step of integration, Δt, to a value computed (automatically) in the present model from an extension of the diffusion number stability criterion [10]. In contrast, the utilization of the implicit method, does not limit the magnitude of the time step (except for considerations of accuracy), but requires a relatively expensive matrix inversion. Both methods predict identical steady state results. Furthermore, if the same Δt values are employed, both methods simulate identical transient behavior and reach the same asymptotic temperature. It was found that the utilization of the implicit method is preferable (from computer–time considerations) in the evaluation of the calorimeter steady–state conditions. On the other hand, a correct simulation of the transient conditions in the calorimeter needs small time steps (of the order of 0.1 seconds) and, therefore, the explicit technique is desirable. Also, a correct evaluation of the temperature profile in the preheater, before the sample is introduced into the calorimeter, requires relatively small time steps (of about one second) and the explicit method was used in this case as well.

In eq. (2.5), the nuclear source term, $Q_{N,i}^{n+1}$ can be a tabulated function of time. The default value of $Q_{N,i}^{n+1}$ is zero during the calorimeter's steady state computations. During the transient computations, $Q_{N,i}^{n+1}$ is assigned a set of constant values according to the heat generation in the corresponding canister's control volumes which are transferred from the preheater (as described later in this section). The electrical source term is continuously updated from the solution of the control equation, as discussed later.

To obtain the steady-state conditions, a convergence criterion is imposed for each CV such that:

$$\left|T_i^{n+1} - T_i^n\right| < \epsilon d_i T_i^n \qquad (2.7)$$

where

ϵ = convergence parameter; default value $\epsilon = 10^{-6}$
d_i = diffusion number defined by: $d_i \equiv \alpha_i \Delta t / \Delta x_i^2$
α_i = diffusity, $\alpha_i = k_i/(\rho_i, c_i)$ and
Δx_i = max (x_{ij}); x_{ij} is the distance between the opposite faces of CV_i.

The control equation (2.3) is also integrated over every CV of interest and over time from t to $t + \Delta t$. The finite difference equation obtained is:

$$Q_{e,i}^{n+1} = Q_{e,i}^n \left\{1 + k_p[T_r - T_i] + \frac{k_i}{t_i}\left[\int (T_r - T_i)dt\right] + k_d\left[(T_r - T_i^{n+1}) - (T_r - T_i^n)\right]\right\} \qquad (2.8)$$

The derivative time was taken to be the same as the computational time step, Δt. The integral time, t_i, is an input parameter of the model. The integration in eq. (2.8) is performed by a trapezoidal rule. This lower order integration technique has been used because the temperature does not change substantially during the transient. The temperature T_i can be evaluated at the times t, $t + \Delta t$ or $t + \Delta t/2$ (default value).

The coupled finite difference equations (2.5) and (2.8) are simultaneously solved at every time step for each control volume of interest. The strategy of computation is as follows:

1. Calculate the steady state conditions of the calorimeter without nuclear heat sources and with an empty canister's chamber. For these calculations, the model provides two options:
   - impose the power of each electrically heated cylinder and find the temperature field along and across the calorimeter (direct problem),
   - impose the reference (set-point) temperature of certain cylinders, for which the electrical power is the dependent variable (inverse problem). This option has always been used in the prediction of the results given in the next section.

   It should be noted that both methods predict identical temperature fields, and electrical powers, as expected.
2. Calculate the canister's temperature field while heated in the preheater, before transferring it to the calorimeter. Also during this step, two options are provided:
   - impose the preheater's reference temperature and calculate the temperature field and the required electrical power supplied to preheater,
   - impose a certain time of preheating and again evaluate the temperature field and the electrical power.
3. Calculate the temperature field of canister during its transfer time from the preheater to the calorimeter. The canister is allowed in this time to transfer heat to the ambient. The transfer time is an input value.
4. Replace the empty canister's control volumes, by those transferred from the preheater and evaluate the transient behavior of the system. During this step we always impose the reference temperatures of certain cylinders and compute the transient behavior of their electrical power supply and temperature field.

Based on the present physical-mathematical model and the strategy presented above, a computer code, CALOR (having almost 4000 FORTRAN statements), has been developed. The computed results are presented and discussed in the next section.

3 Results and Discussion

The calorimeter simulation model was applied to study the transient response of a hypothetical fast air-bath calorimeter. The calorimeter is designed to measure the thermal power emitted by Pu-containing samples. Its most important design characteristic is that the sample chamber is operated in an isothermal mode. The sample chamber is kept at a constant temperature (48 °C) by a PID (proportional-integral-differential) controller which sets the chamber heater power using electronic-feedback circuits. When the chamber temperature departs from its set-point of 48 °C , an error signal directs electrical power to a copper heating coil wrapped arround the sample chamber. The electrical power history is the only measured parameter used in the data analysis and is normally used by the calorimeter data aquisition system to predict the sample power.

In fast calorimetry, the sample is preheated before being introduced into the calorimeter chamber. The preheater temperature is normally adjusted, via a servo-controlled electrical heating coil, to match as closely as possible the calorimeter chamber temperature. Since the sample is brought to thermal equilibrium in the preheater (i.e., develop a steady spatial temperature profile), a long preheat time is necessary before the sample is transferrd to the calorimeter chamber. Modeling the preheater response is, therefore, important for optimizing the calorimeter response.

Figure 1 is a schematic of the numerical model of the calorimeter. The model uses 70 control volumes to closely represent the heaters, the sample cavity, the outer calorimeter container and the insulation materials. The sample chamber is represented by 3 axial volumes (vols. 31, 41, and 51) surrounded by the inner heater (vols. 22, 32, 42 and 52) made of a copper coil wrapped on an Al cylinder. The heating coils are insulated by layers of epoxy–stycast (ES–1266). Electrical power is normally applied to the three heating elements and to the outer Al container to minimize the effect of possible variations in the ambient conditions.

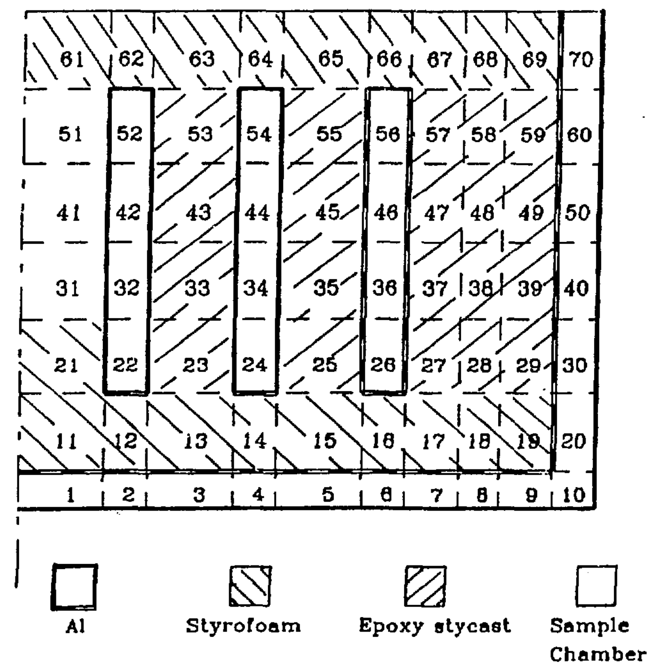

Figure 1. Mesh Set-Up for Numerical computations.

Each control volume of the numerical model is considered to exchange heat with its neighboring volumes by conduction and radiation and, at the boundaries of the system, by convection and radiation. Heat transfer in complicated geometries can, thus, be conveniently simulated by proper choice of the number and shapes of the control volumes. The simulation scheme shown in Fig. 1 provides an approximate representation of an *ANL* air–bath system for parametric studies of the main design and operational factors influencing the system's response time and accuracy. To demonstrate some of the model capabilities, it was applied to study the effect on the system behavior of the source homogeneity and of the setting of the power control system. Three basic cases were analysed as follows:

Case 1: A 4.4 Watt Pu–bearing source was assumed to be unifomly distributed in the lower 1/3 section of the canister (CV 31). The canister was assumed to be transferred within 5 s to the calorimeter chamber after reaching an equilibrium temperature in the preheater. During this time it cools by convection and radiation to the surrounding.

Case 2: The same as case 1 but with the source uniformly distributted in the middle 1/3 of the canister's volume (CV 41).

Case 3: The same source was assumed to occupy the upper 1/3 of the canister's volume (CV 51).

The effect of the preheater temperature was studied by calculating each case twice; once with a preheater temperature of 48 °C and the other with a preheater temperature of 47.5 °C , i.e., 0.5 °C below the calorimeter chamber equilibrium temperature. To demonstrate the importance of the setting of the controller coefficients, case 3 was recalculated with an integral coefficient of 0.4 which is higher by a factor of 4 than the normal setting of 0.1.

Figure 2 shows the electrical power history for case 1. The solid and dashed lines represent the system's response for the two preheater temperatures (48 and 47.5 °C) respectively. In both cases the sample was assumed to be in equilibrium conditions before being transferred to the calorimeter chamber. It is noticed that when the sample temperature is lower than the calorimeter temperature the power rises in the first minute before descending to a new assymptotic value. On the other hand, a continuous power decay was obtained for the hotter sample temperature. The assymptotic power value, however, does not depend on the initial sample temperature. The difference between the initial and final electrical power is slightly less than the sample power resulting from some uncontrolled heat losses in the calorimeter. The heat losses are typically accounted for during the calibration tests of the system. In case 1 the power losses are shown to be less than 1%.

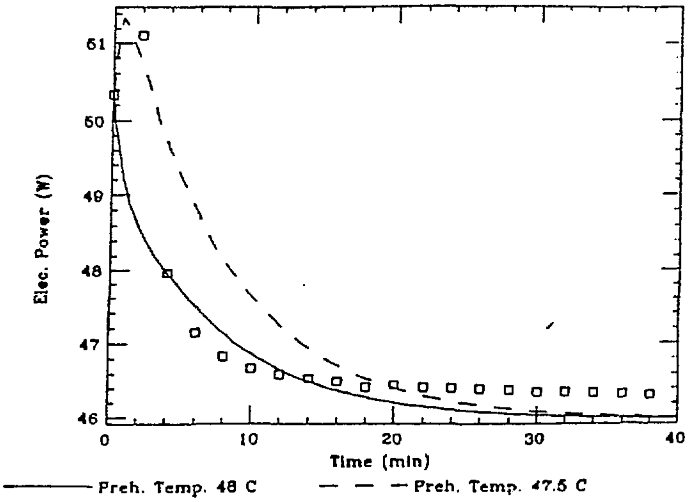

Figure 2. Power History, Source Position–Bottom; Integral Coefficient 0.1.

The data points in Fig. 2 were measured in a 40-Watt calorimeter which is similar (but not identical) to the model shown in Fig 1. The sample was preheated for 16 hr and its surface temperature reached an equilibrium temperature of 47 °C . The initial calorimeter chamber temperature was 47.87 °C and the initial equilibrium power was 50.3 Watt. The power rises to above 51 Watt and then drops within less than an hour to a steady level of 46.17 Watt. The deviations are caused by the different setting of the control system and differences in geometry between the simulated and the actual system.

For purpose of code varification and comparison with experimental data, we have also examined the system's behavior when an empty canister (filled with air), initially heated to 48 °C and 47.5 °C is introduced into the calorimeter. As expected, in both cases the electrical power remained almost constant. A slight power increase, by about 0.01%, was observed after 1 hr of transient due to heat losses.

Simulated power histories for cases 2 and 3 are plotted in Figs 3 and 4, respectively. The power peak obtained when a relatively cold sample is introduced to the calorimeter chamber is higher when the source is placed at the top of the canister (case 3) relative to cases 1 and 2 in which the source is at the bottom or the center of the canister. This is probably due to the larger heat losses from the top section of the modelled calorimeter relative to its lower part. Uncontrolled heat losses from the upper section of the calorimeter also explain the higher assymptotic power value obtained when the Pu sample is at the top of the canister. The electrical power bias (i.e., the difference between the sample power and the electrical power drop) is predicted to be more than 7% when the source is distributed at the top section of the

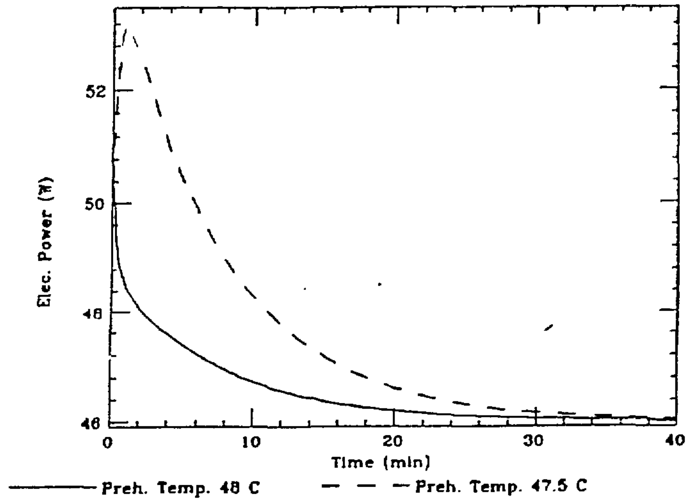

Figure 3. Power History, Source Position–Center; Integral Coefficient 0.1.

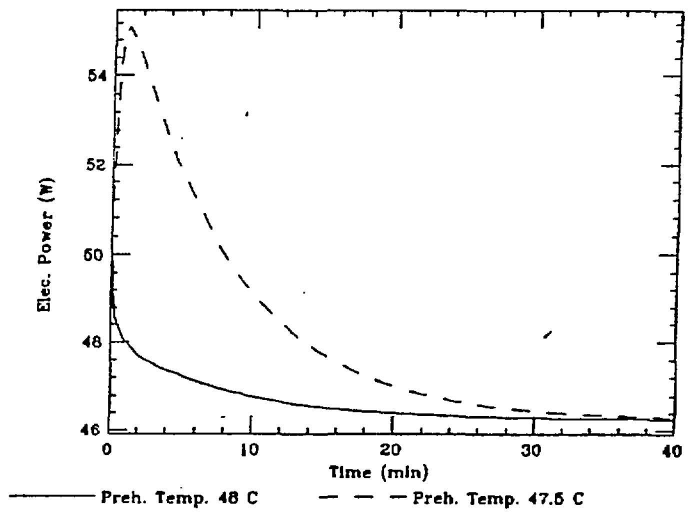

Figure 4. Power History, Source Position–Top; Integral Coefficient 0.1.

canister compared to about 1.5% when the source is at the center of the canister and less than 1% when the source is at the bottom. It should be noted that in the present model, the control volumes above the one with the source are assuned empty (filled with air), having a much smaller thermal conductivity than the Al shot. Therefore, when the source is at the bottom of the canister it is insulated from the top calorimeter plug by the air above the can. On the other hand, when the source is at the top of the canister, the canister is filled with Al shot and consequently the heat loss from the upper styrofoam plug is enhanced. The smaller electrical power drop obtained for a source at the top indicates the importance of the insulation of the upper section of the calorimeter.

The effect on the power history of the control system setting is demonstrated in Figs. 5 and 6 for a source at the bottom section of the canister. Increasing the integral controller coefficient increases the early power overshoot (when a relatively cold sample is measured) but brings the power faster to its final level. When the sample temperature is close to the initial calorimeter temperature (48 °C), increasing the integral controller coefficient speeds up the system response. Using an integral control coefficient of 0.4, causes the electrical power to drop to within 2% of its equilibrium value within less than 10 min. It should be noted, however, that using a too large integral coefficient may cause the power to oscillate and, in some cases, to be unstable.

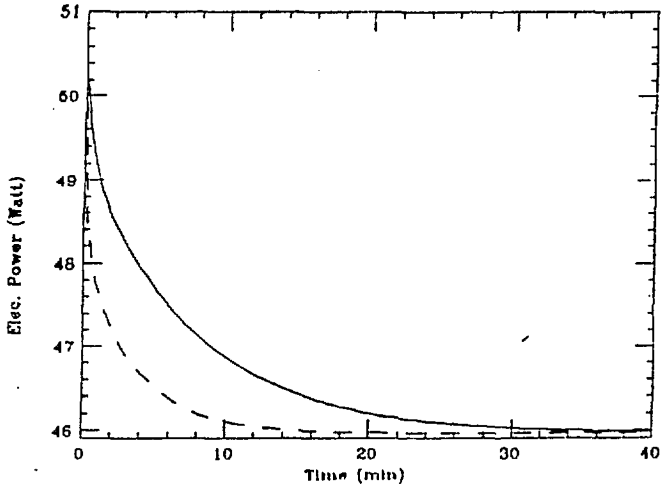

Figure 5. Effect of Controller Setteing On Power History, Source Position–Bottom; Chamber Temperature 48 °C .

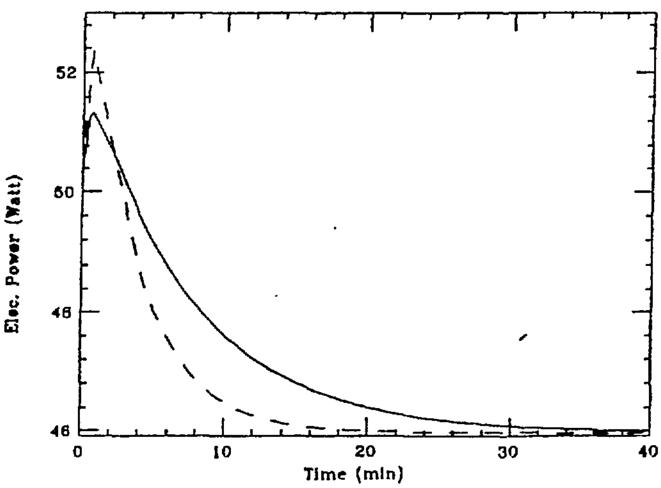

Figure 6. Effect of Controller Setteing On Power History, Source Position–Bottom; Chamber Temperature 47.5 °C .

4 Conclusions

A 3–dimensional heat transfer model has been developed to analyze the design and operational characteristics of calorimetric assay systems.

The model is written in a modular manner which makes it suitable for the analysis of complicated heat transfer configurations. Work is underway to use the program to study alternative system configurations and modes of operation in order to arrive at an optimal design of a fast calorimetric system.

References

[1] M. F. Duif, J. R. Wetzel and J. F. Lemming, "Calorimetry Design considerations for Scrap Assay", Trans. Am. Nucl. Soc., 50, 170 (1985).

[2] C. L. Fellers and P. W. Seabaugh, "Real–Time Prediction of Calorimeter Equilibrium", Nucl. Instr. Methods, 163, 499 (1979).

[3] R. B. Perry et al., "The Bulk Assay Calorimeter", ANL-NDA-9 ISPO-14, Argonne National Laboratory (1982).

[4] Richard L. Mayer II, "Modeling Response Variation for Radiometric Calorimeters", Proc. INMM, XV,237 (1986).

[5] Richard L. Mayer II, "Application of Prediction of Equilibrium to Servo-Controlled Calorimetry Measurements", Proc. INMM XVI, 364 (1987).

[6] D. R. Rogers (Ed.) "Handbook of Safeguards Measurement Methods", MLM-2855, NUREG/CR-2078 (1981).

[7] S. Fiarman and R. B. Perry, "Attributes Measurements by Calorimetry in 15 to 30 Minutes", Proc. INMM XVI, 754 (1987).

[8] S. Fiarman and R. B. Perry, "Field Test Results of Fast Calorimetry Using the Argonne Bulk Calorimeter at Rocky Flats and TA-55", TSO 87-11 Information Report, Brookhaven National Laboratory (1987).

[9] R. B. Perry and S. Fiarman, "Recent Development in Fast Calorimetry", Proc. INMM XVII, 697 (1988).

[10] P. J. Roache, "Computational Fluid Dynamics", Hermosa Publishers, 1982.

[11] W. S. Janna, "Engineering Heat Transfer", PWS Publishers, 1986.

DISCLAIMER